Observation of Superradiance by Nonlocal Wave Coupling of Light and Excitons in CuCl Thin Films

Masayoshi Ichimiya,[1,2,*] Masaaki Ashida,[1,2] Hideki Yasuda,[1,3] Hajime Ishihara,[1,3] and Tadashi Itoh[1,2]

[1]*CREST-JST, 4-1-8 Honmachi, Kawaguchi 332-0012, Japan*

[2]*Department of Materials Engineering Science, Osaka University, Osaka 560-8631, Japan*

[3]*Department of Physics and Electronics, Osaka Prefecture University, Osaka 599-8631, Japan*

(Received 24 September 2008; published 14 December 2009)

We report the observation of a remarkably strong coupling between light and a multinode-type exciton. The observed radiative decay time reaches the order of 100 fs, which is much faster than the dephasing process of nonradiative scattering. In this high-speed superradiance, the light wave and the excitonic wave in a high-quality thin film form a harmonized wave-wave coupling over a range of multiple wavelengths. This mechanism contradicts the conventional physical description of light-matter interaction based on the long-wavelength approximation.

DOI: 10.1103/PhysRevLett.103.257401 PACS numbers: 78.67.Pt, 71.35.−y, 71.36.+c, 82.53.Mj

The oscillator strength is a standard measure used to describe the coupling strength between a photon and the quantum state of the matter. The concept of giant oscillator strength by Rashba and Gurgenishvili [1] stimulated research into controlling light-matter coupling by manipulating excitonic center-of-mass (c.m.) wave functions, which led to the conclusion of a size-linear enhancement of the oscillator strength [2–5]. The concept of the oscillator strength has been based on the long-wavelength approximation (LWA), wherein the spatial structure of the light wave is neglected by assuming a much longer wavelength of resonant light (λ) than the excitonic coherent length (ξ) as shown in Fig. 1(a). Under this framework, the above size-linear enhancement is saturated by ξ, because of the violation of c.m. confinement due to the dephasing, or λ, because of the phase mismatch between the lowest optically permitted exciton and the light wave.

In this Letter, we report the observation of a light-exciton coupling beyond the concept of the oscillator strength under the LWA. Our theoretical analysis clearly elucidates that the wave-wave coupling between the light and the extended exciton over multiple wavelengths, which also exhibits a size-dependent increase, eventually causes radiative decay that is much faster than the dephasing process.

The observation of an exciton with a very large c.m. wave vector in GaAs thin films has recently been reported [6], where the non-LWA coupling was observed by a skillful technique, although this coupling is not very large because of the phase mismatch between the radiation and excitons. On the other hand, a peculiar nonlinear response contradicting the LWA was reported, wherein the ''size-resonant'' enhancement of the nonlinear signal arising from the ''nondipole-type'' excitonic state [$n = 2$ exciton in Fig. 1(a)], which is normally an optically forbidden state, was predicted and observed in GaAs thin films [7–9]. This effect is based on phase-matched coupling, and is expected to lead to a situation where the coupling between the light wave and the extended ''multinode-type'' excitonic wave is formed over several wavelengths [as illustrated in Fig. 1(b)]. Such a coupling has not been considered as an experimental reality so far in spite of the theoretical arguments based on the crossover issue between the superradiance regime and the bulk polariton regime [10,11].

Recently, we reported an experiment of two-pulse degenerate four-wave mixing (DFWM) implying the coupling between light and a multinode-type exciton [12]. However, the two-pulse DFWM provides information about the decay time that is determined by the sum of the population relaxation rate and the dephasing rate, and thus, definite evidence of fast radiative decay cannot be obtained by this method. In the present work, we have observed three-pulse DFWM [transient grating (TG) configuration] that provides information about the pure population relaxation times. A clear theoretical analysis for this result successfully reveals existence of wave-wave coupling between light and an exciton and its femtosecond radiative decay for the first time.

To demonstrate the wave-wave coupling, we prepare high-quality CuCl thin films with a very small phase decay

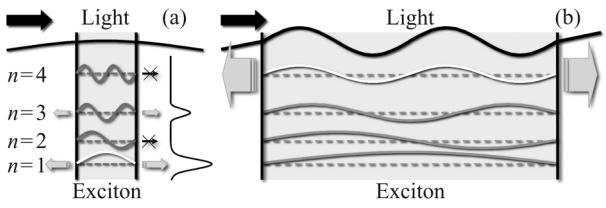

FIG. 1. Images of the coupling between light and excitons in the LWA regime (a) and the harmonized wave-wave coupling between a multinode-type exciton and light (b). The black curve on the right in (a) is a schematic spectrum. The states most strongly coupled with the light field are indicated in white.

constant (Γ) of less than 1 meV by molecular-beam epitaxy (MBE) [13]. The excitons of I-VII semiconductors have very strong radiative coupling per unit cell volume [14]. Thus, their wave-wave coupling is expected to result in an extremely large radiative shift [15,16] and a width [15] on the order of tens of meV when the film thickness is above 100 nm, which corresponds to a radiative decay time of a few tens of femtoseconds. A particularly interesting point is that such a decay time is significantly less than the excitonic dephasing time, which is normally on the order of picoseconds [17,18]. This interchange would lead to an unconventional situation where the coherent optical response is completed before the excitation is affected by the phase decay. That is, in this inverted situation, even the dephasing process would not be able to limit the size-dependent increase in the light-matter coupling.

In our experiment, CuCl thin films were mounted in a helium flow cryostat and cooled to below 10 K. DFWM was measured using the second harmonic of a mode-locked Ti:sapphire laser, whose repetition rate and pulse duration were 80 MHz and 110 fs, respectively. The photon energy of the pulse was tuned to approximately the transverse exciton energy in CuCl (3.2022 eV) and the spectral width was approximately 20 meV, which covered the exciton resonance region. The light was split into two or three (TG configuration) pulses and all of them were focused onto the same spot on the sample surface. In the DFWM measurements, the polarizations of the two pulses were parallel, and in the TG configuration, the polarization of the probe pulse was perpendicular to that of the parallel-polarized pump pulses. The signal light was transmitted through an optical fiber to a monochromator equipped with a CCD. The spectral resolution was better than 0.08 meV. The film thickness at the measured spot was derived by fitting to the reflection spectrum measured using the same geometry and excitation light as those in the measurement of DFWM.

For the theoretical analysis, we consider the excitonic c.m. motion confined within a thin film whose direction of thickness is along the z-axis. Since the Bohr radius is much smaller than the film thickness (6–7 Å for a Z_3 exciton in CuCl), we explicitly treat only the degree of freedom of the c.m. motion. Within a subspace of a given wave vector parallel to the film surface $K_{\|}$, we, respectively, consider the following eigenfunctions and eigenenergies for the basis of c.m. motion of excitons along the z axis: $\psi_n(z) = (2/d)^{1/2} \sin K_n z$ and $E_n = \hbar^2(K_n^2 + K_{\|}^2)/2M$, where d is the film thickness, K_n is the quantized wave number perpendicular to the film surface whose quantization condition is given as $K_n = n\pi/d$ for a positive integer n, and M is the effective mass of the exciton.

In the linear response calculation, we consider the nonlocal relationship between the induced polarization $P(z)$ and the electric field $E(z)$ in accordance with the method in [15]. The induced polarization can be expanded as $P(z) = \sum_n X_n(\omega)\psi_n(z)$ using the bases of excitonic c.m. motion [15]. The spectrum of the expansion coefficient $|X_n(\omega)|^2$ includes information on the radiative shift and width of the nth excitonic state (as shown in Fig. 2).

To calculate the DFWM signal, we numerically solve the simultaneous equations of motion for the source current density $j(z, t)$ and the vector potential $A(z, t)$ written in the Coulomb gauge as functions of time t by the Runge-Kutta method. $A(z, t)$ is described with the standard microscopic Maxwell equation including source current density $j(z, t)$, which is given as the quantum mechanical average of the current density operator $\hat{J}(z)$, namely $j(z, t) = \sum_{nm}\rho_{mn}\langle n|\hat{J}(z)|m\rangle$, where $\{|n\rangle\}$ denotes the eigenstates of the matter system and ρ_{mn} are the elements of the density matrix expanded using these bases. The motion of ρ_{mn} is determined by the equation

$$\dot{\rho}_{mn} = (i/\hbar)(\epsilon_m - \epsilon_n)\rho_{mn} + (i/c\hbar) \times \Big[\sum_l \Big\{\rho_{lm}\int\langle n|\hat{J}(z)|l\rangle A(z, t)dz - \rho_{nl}\int\langle l|\hat{J}(z)|m\rangle A(z, t)dz\Big\}\Big], \quad (1)$$

where $\{\epsilon_n\}$ denotes the eigenenergies of the states $\{|n\rangle\}$. From the solution of $A(z, t)$ obtained by assuming a negligibly small $K_{\|}$, we extract the component of the DFWM signal corresponding to the observed signal for both two-

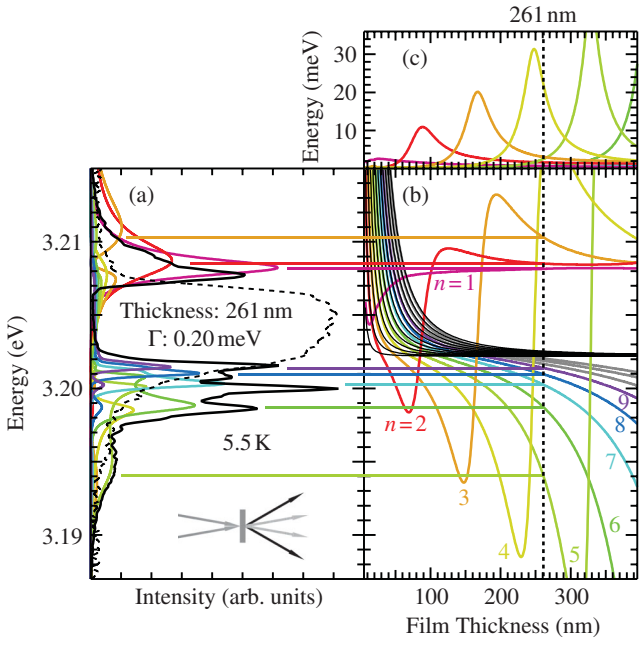

FIG. 2 (color). (a) Observed DFWM spectrum in a CuCl thin film (black line) and calculated induced-polarization spectra. The dashed curve indicates the linear absorption spectrum. The inset schematic diagram shows the configuration of this measurement (two-pulse DFWM). (b) Film thickness dependences of calculated eigenenergies including the radiative shift and uncoupled excitonic modes (black lines) [15]. (c) Film thickness dependence of calculated radiative width [15].

pulse and three-pulse configurations by a numerical technique. Furthermore, by the Fourier transformation of the calculated signals for various delay times, we can obtain the delay time profile at any energy point. As the origins of nonlinearity, we consider the state filling due to the Pauli exclusion effect and the exciton-exciton interaction. Discretizing the medium and assuming the one-dimensional transfer reduced from the effective mass M, we introduced an attractive interaction between excitons at neighboring sites, which yields biexciton and free two-exciton states. In the present analysis, the biexciton resonance does not appear in the observed energy region because the biexcitonic binding energy of CuCl is large (32 meV). Also, by varying a fitting parameter multiplied by the coupling coefficients between excitons and two-exciton states, we find no significant effect of free two-exciton states within the degree of precision of the present experiments because it changes the results by the amount of the nonlinear portion. Thus, in the present discussion, we focus on the effects of the one-exciton resonance.

For both linear and nonlinear calculations, the phase decay constant of excitons (Γ) is phenomenologically introduced and treated as a fitting parameter. Since the linear spectrum is very sensitive to Γ, the film thickness and the value of Γ can be determined with satisfactory accuracy by linear spectral fitting, and we use this value in the DFWM calculation. For the other parameters, we use $M = 2.28m_0$, $\varepsilon = 5.59$ and 3.2022 eV for the energy of the bulk transverse exciton, where m_0 and ε are the electron mass and the background dielectric constant, respectively. Because of the self-consistent treatment of $A(z, t)$ [$E(z, t)$] and $j(z, t)$ [$P(z, t)$] in the above calculations, the size-dependent radiative correction (shift and width), or the radiative decay-time profile automatically appears in the result. Note that the only fitting parameters in the present calculation are d and Γ.

A typical DFWM spectrum with a two-incident-beam configuration is shown in Fig. 2(a), where a CuCl film with a thickness of 261 nm and Γ of 0.20 meV exhibits several peaks. The temperature of the sample was maintained at 5.5 K and the delay time between two pulses was set to zero in the measurement of the DFWM spectrum. The density of photogenerated carriers is estimated to be 7.0×10^{15} cm^{-3}. In Figs. 2(b) and 2(c), the calculated radiative shift and width exhibit complicated nonmonotonic behavior with increasing thickness, which reflects the change in the phase relation between the excitons and the light waves with size, and their maximum values increase. Note that the observed peaks are in good agreement with the calculated eigenenergies for $n = 5$–9 at 261 nm [vertical dotted line in Fig. 2(b)]. Furthermore, the photon energy and spectral width for each component in the spectrum closely reflect the shape of the calculated induced-polarization spectrum for the corresponding eigenstate [19]. Both the linear and nonlinear spectra are well reproduced by the same Γ value (no figure for the linear spectrum), which indicates that there is no appreciable effect of the excitation-induced dephasing at the present excitation density for this material. Thus, we have succeeded in experimentally elucidating the systematic level scheme of the coupled system of photons and multinode-type excitons for thicknesses above hundreds of nanometers. It should be noted that such an excellent agreement between the calculated and experimental results can be obtained for samples with different thicknesses provided they are successfully fabricated. For example, Fig. 3 shows the result of DFWM for a thinner 190-nm-thick film, where the eigenenergies and spectral shape are also well explained by the calculated mode diagram and induced polarization. In this case, we observe broad spectral shapes of the components at approximately 3.195 eV and 3.209 eV that reflect the induced-polarization spectra corresponding to the eigenstates for $n = 4$ and 2, whose radiative widths reach 2.5 and 2.3 meV, respectively.

As shown in Figs. 2 and 3, some higher-order states with broad peaks are observed. If these widths actually reflect the radiative decay time, they appear to be much faster than the phase decay time of these samples evaluated from Γ determined by fitting to the linear spectra. To verify this point, the dependence of DFWM on the time delay of the probe pulse is measured with the TG configuration, where the pure population decay time should be reflected in the result [20]. The decay profiles at three energy points, namely, at energies corresponding to the $n = 5$, $n = 1$, 2 and $n = 3$ states are plotted in Figs. 4(a)–4(c), respectively. The dashed lines represent the fitting functions, which are exponential functions convoluted by the excitation laser profile, where the time constants of the fastest components derived from the radiative width in Fig. 2(c) are substituted into the fitting functions. The results exhibit two noteworthy characteristic features. The first is an exceptionally short radiative decay time of as low as 100 fs, which is several orders of magnitude shorter than the typical excitonic radiative decay time. The second is a clear beat structure in these decay curves. With regard to the first point, it is found that the fastest component in each observed curve is consistent with the value derived from the calculated radiative width of the corresponding state. For

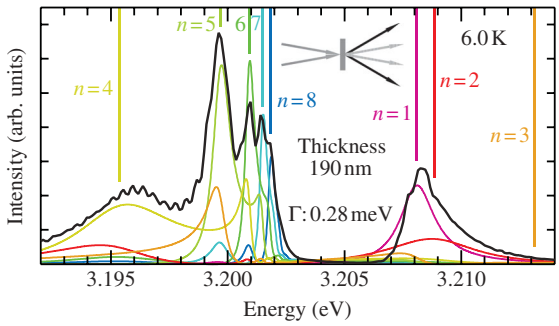

FIG. 3 (color). Comparison between a DFWM spectrum and induced-polarization spectra. The vertical solid lines indicate eigenenergies for a thickness of 190 nm, which are derived from Fig. 2(b).

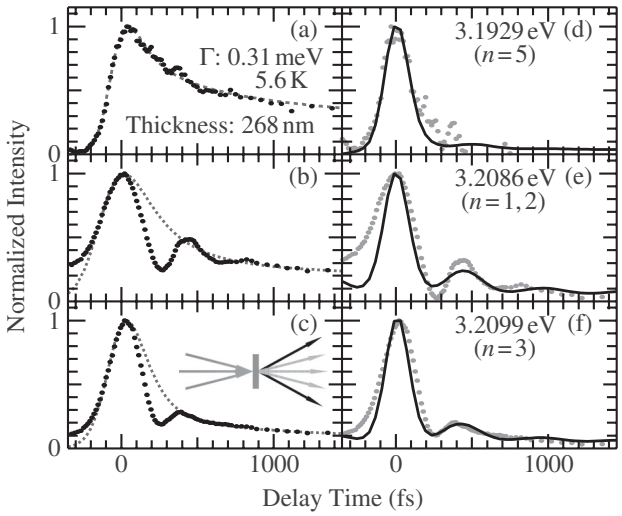

FIG. 4. (a)–(c) Observed delay time dependence of the TG signal intensity in a CuCl thin film. The inset schematic diagram shows the TG configuration (three-pulse DFWM). (d)–(f) Delay time dependence of the TG signal intensity calculated by a real-time analysis (solid lines). The gray points indicate the fast components, among which those with long time constants are subtracted from the measured values shown in (a)–(c).

example, the spectral widths of the eigenstates assigned by fitting with the calculated induced-polarization spectra for $n = 5$ and $n = 3$ are 3.2 and 2.9 meV, respectively, at a thickness of 268 nm, as shown in Fig. 2(c). The decay times corresponding to these values are 103 and 115 fs for the $n = 5$ and $n = 3$ states, respectively. If components with a long time constant, which is evaluated from the above fitting, are subtracted from the measured values, each decay profile agrees well with the result of the real-time calculation, as shown in Figs. 4(d)–4(f). Regarding the second point, the clear beat structures in the decay curves reveal the high excitonic coherence over the entire volume of the sample up to higher-order states, despite a thickness of several hundred nanometers. The observed beat structures in Figs. 4(a)–4(c) have beat frequencies of 400–500 fs, which are attributed to the quantum interference between the lower and higher excitonic states, which are separated by a large energy gap due to the enormous radiative shift. The beat frequency caused by the quantum interference between excitonic states with an energy separation of ΔE can be obtained from the equation $T = h/\Delta E$ (h represents Planck's constant). For example, in the case of a thickness of 268 nm, the energy separation between the excitonic states of $n = 1$ and 7 is obtained from the theoretical calculation [Fig. 2(b)] to be about 8.1 meV, which corresponds to a beat frequency of 511 fs, and for the excitonic states of $n = 2$ and 6, the energy separation is about 10.1 meV and the beat frequency is 409 fs. These values are in good accordance with the observed beat frequencies. Thus, we have successfully verified that the harmonized wave-wave coupling yields exceptionally high-speed superradiance that is much faster than the normal dephasing process. It should be emphasized that this ultrafast decay is peculiar to the superradiant thickness regime that is separated from the time-of-flight regime [21] by the clearly defined transition thickness (see Ref. [22] for details).

In conclusion, the present results indicate the possibility of new avenues in designing light-matter coupling by manipulating the spatial interplay between the waves of electronic excited states and light, which is in striking contrast with the conventional scenario wherein the spatial degrees of freedom of these waves are treated in hierarchically different regimes. Furthermore, the sample structure, size regime and measurement method are fairly conventional in this study. We have thus provided a clear example showing that the straightforward control of the size and quality of conventional structured materials can considerably enhance the degree of freedom enabling the development of novel material functions. Hence, further studies on similar effects involving other types of materials with a large excitonic effect, such as ZnO, GaN and organic materials, are required in order to explore the hidden potential of photonic functions.

*ichimiya@laser.mp.es.osaka-u.ac.jp

[1] E. I. Rashba and G. E. Gurgenishvili, Sov. Phys. Solid State **4**, 759 (1962).
[2] E. Hanamura, Phys. Rev. B **37**, 1273 (1988).
[3] T. Takagahara, Phys. Rev. B **39**, 10 206 (1989).
[4] A. Nakamura, H. Yamada, and T. Tokizaki, Phys. Rev. B **40**, 8585 (1989).
[5] T. Itoh *et al.*, Solid State Commun. **73**, 271 (1990).
[6] G. Göger *et al.*, Phys. Rev. Lett. **84**, 5812 (2000).
[7] H. Ishihara and K. Cho, Phys. Rev. B **53**, 15 823 (1996).
[8] K. Akiyama *et al.*, Appl. Phys. Lett. **75**, 475 (1999).
[9] H. Ishihara *et al.*, Phys. Rev. Lett. **89**, 017402 (2002).
[10] J. Knoester, Phys. Rev. Lett. **68**, 654 (1992).
[11] G. Björk *et al.*, Phys. Rev. B **52**, 17 310 (1995).
[12] M. Ichimiya *et al.*, Phys. Status Solidi B **243**, 3800 (2006).
[13] A. Kawamori, K. Edamatsu, and T. Itoh, J. Cryst. Growth **237–239**, 1615 (2002).
[14] T. Mita, K. Sotome, and M. Ueta, J. Phys. Soc. Jpn. **48**, 496 (1980).
[15] H. Ishihara, J. Kishimoto, and K. Sugihara, J. Lumin. **108**, 343 (2004).
[16] A. Syouji *et al.*, Phys. Rev. Lett. **92**, 257401 (2004).
[17] D. K. Shuh *et al.*, Phys. Rev. B **44**, 5827 (1991).
[18] E. Vanagas *et al.*, Phys. Rev. B **63**, 153201 (2001).
[19] It has been analytically shown that the DFWM spectrum generated by an ultrashort pulse should reflect the spectral shape of $|X_n(\omega)|^2$ (unpublished result).
[20] T. Yajima and Y. Taira, J. Phys. Soc. Jpn. **47**, 1620 (1979).
[21] Y. Masumoto, S. Shionoya, and T. Takagahara, Phys. Rev. Lett. **51**, 923 (1983).
[22] M. Bamba and H. Ishihara, Phys. Rev. B **80**, 125319 (2009).